UC Davis
UC Davis Previously Published Works

Title

Hyperamylinemia Contributes to Cardiac Dysfunction in Obesity and Diabetes

Permalink

Journal

ISSN

Authors

Despa, Sanda
Margulies, Kenneth B
Chen, Le
et al.

Publication Date

DOI

Peer reviewed

Hyperamylinemia Contributes to Cardiac Dysfunction in Obesity and Diabetes : A Study in Humans and Rats

Sanda Despa, Kenneth B. Margulies, Le Chen, Anne A. Knowlton, Peter J. Havel, Heinrich Taegtmeyer, Donald M. Bers and Florin Despa

The online version of this article, along with updated information and services, is located on the World Wide Web at:

http://circres.ahajournals.org/content/110/4/598

Data Supplement (unedited) at:

http://circres.ahajournals.org/content/suppl/2012/01/24/CIRCRESAHA.111.258285.DC1.html

---

Permissions: Requests for permissions to reproduce figures, tables, or portions of articles originally published in *Circulation Research* can be obtained via RightsLink, a service of the Copyright Clearance Center, not the Editorial Office. Once the online version of the published article for which permission is being requested is located, click Request Permissions in the middle column of the Web page under Services. Further information about this process is available in the Permissions and Rights Question and Answer document.

Reprints: Information about reprints can be found online at:
http://www.lww.com/reprints

Subscriptions: Information about subscribing to *Circulation Research* is online at:
http://circres.ahajournals.org//subscriptions/

Hyperamylinemia Contributes to Cardiac Dysfunction in Obesity and Diabetes
A Study in Humans and Rats

Sanda Despa, Kenneth B. Margulies, Le Chen, Anne A. Knowlton, Peter J. Havel,
Heinrich Taegtmeyer, Donald M. Bers, Florin Despa

Rationale: Hyperamylinemia is common in patients with obesity and insulin resistance, coincides with hyperinsulinemia, and results in amyloid deposition. Amylin amyloids are generally considered a pancreatic disorder in type 2 diabetes. However, elevated circulating levels of amylin may also lead to amylin accumulation and proteotoxicity in peripheral organs, including the heart.

Objective: To test whether amylin accumulates in the heart of obese and type 2 diabetic patients and to uncover the effects of amylin accumulation on cardiac morphology and function.

Methods and Results: We compared amylin deposition in failing and nonfailing hearts from lean, obese, and type 2 diabetic humans using immunohistochemistry and Western blots. We found significant accumulation of large amylin oligomers, fibrils, and plaques in failing hearts from obese and diabetic patients but not in normal hearts and failing hearts from lean, nondiabetic humans. Small amylin oligomers were even elevated in nonfailing hearts from overweight/obese patients, suggesting an early state of accumulation. Using a rat model of hyperamylinemia transgenic for human amylin, we observed that amylin oligomers attach to the sarcolemma, leading to myocyte Ca^{2+} dysregulation, pathological myocyte remodeling, and diastolic dysfunction, starting from prediabetes. In contrast, prediabetic rats expressing the same level of wild-type rat amylin, a nonamyloidogenic isoform, exhibited normal heart structure and function.

Conclusions: Hyperamylinemia promotes amylin deposition in the heart, causing alterations of cardiac myocyte structure and function. We propose that detection and disruption of cardiac amylin buildup may be both a predictor of heart dysfunction and a novel therapeutic strategy in diabetic cardiomyopathy. (*Circ Res*. 2012;110:598-608.)

Key Words: hyperinsulinemia ■ hyperamylinemia ■ diabetic cardiomyopathy ■ calcium ■ HIP rat ■ UCD-T2DM rat

One-third of adults and 17% of children in the United States (from the National Center for Health Statistics, 2009) are currently obese and at high risk of developing both type 2 diabetes and cardiovascular disease.[1–3] Progression to overt type 2 diabetes may accelerate pathological changes in heart structure and function,[4–7] independent of confounding factors such as coronary artery disease and hypertension.[1–3] It is assumed[1] that increases in body fat can affect the body's response to insulin, potentially leading to insulin resistance and subsequent impaired glucose and lipid homeostasis. As

such, insulin resistance is unequivocally associated with heart disease.[1–10] However, the myocardial insulin responsiveness in diabetic patients is surprisingly intact,[11,12] suggesting that factors secondary to insulin resistance may critically contribute to cardiac dysfunction in type 2 diabetes.[5,9,10] In addition to hyperglycemia and dyslipidemia, patients with obesity and insulin resistance present also hyperinsulinemia and hyperamylinemia.[13–15] Whereas the hyperinsulinemic response prevents a large fraction of insulin resistant patients from developing type 2 diabetes,[1] the coincident hyperamylinemia

© 2012 American Heart Association, Inc.

Circulation Research is available at http://circres.ahajournals.org

DOI: 10.1161/CIRCRESAHA.111.258285

leads to proteotoxicity and amyloid deposition.[13,14] More than 95% of patients with type 2 diabetes stain positive for amylin amyloids in pancreatic islets.[14] Amylin deposition was also found in kidneys of obese and type 2 diabetic patients.[16] Recently,[17,18] we hypothesized that hyperamylinemia may favor cardiac amylin accumulation,[17] causing alterations of myocyte structure and function in ways that may contribute to progressive heart failure.[18]

Amylin is a 4-kDa hormone coexpressed and cosecreted with insulin by pancreatic β-cells.[13,14] Human amylin, also known as islet amyloid polypeptide (IAPP), has aggregation properties similar to prions and amyloidogenic proteins that are associated with neurodegenerative diseases.[19] At high secretion rates, amyloidogenic proteins readily form oligomers, fibrils, and amyloid plaques. It is increasingly recognized that soluble oligomers rather than fibrils and plaques are the most toxic species of amyloids.[20–28] They attach to cellular membranes causing Ca^{2+} dyshomeostasis, cell dysfunction, and apoptosis.[20–28] Previous data[27,28] indicated that cardiac myocyte–restricted expression and accumulation of amyloidogenic peptides, such as polyglutamine[27] or presenilin,[28] can induce cytotoxicity and heart failure in mice. Presenilin oligomers coimmunoprecipitated with sarcoplasmic reticulum Ca-ATPase (SERCA) and altered Ca^{2+} handling in cardiac myocytes.[28]

To clarify whether amylin builds up in the heart and whether this could be associated with cardiac failure in obesity and type 2 diabetes, we assessed amylin deposition in hearts from lean, obese, and type 2 diabetic humans, with and without heart failure. Using a "humanized" rat model of hyperamylinemia, we examined changes in cardiac structure and function in relation with cardiac amylin accumulation.

Methods

Detailed procedures, description of human tissue specimens and animal models are included in the online-only Data Supplement.

Human Tissue Specimens

Failing hearts from obese, type 2 diabetic, and nondiabetic patients were obtained at the time of orthotopic heart transplantation at the Hospital of University of Pennsylvania. Nonfailing hearts from obese and lean individuals are from organ donation. Tissue specimens were obtained with institutional review board approval. Inclusion in tissue-based studies was not restricted on the basis of age, sex, race, or ethnic status. Heart failure etiology, body mass index, age, sex, and state of diabetes with respect to dependence on insulin and/or oral hypoglycemic agents of all cases studied here are summarized in Online Table I.

Experimental Animals

Studies were approved by the University of California, Davis, Animal Research Committee. Because rodent amylin is not amyloidogenic and rodents do not accumulate amylin amyloids,[29] most rodent models of type 2 diabetes are not adequate for this study. We used Sprague-Dawley (SD) rats transgenic for human amylin in the pancreatic β-cells (HIP rats).[30] HIP rat breeding pairs were kindly provided by Pfizer. HIP rats show hyperamylinemia, leading to amylin deposits in pancreatic islets and gradual decline in β-cell mass.[31] They develop insulin resistance at 5 months of age and diabetes by 10 months of age.[31] As negative controls, we used obese insulin-resistant rats expressing only wild-type, nonamyloidogenic

Non-standard Abbreviations and Acronyms	
BNP	brain natriuretic peptide
HDAC	histone deacetylase
HIP rats	type 2 diabetic rat model transgenic for human amylin
IAPP	islet amyloid polypeptide
NFAT	nuclear factor of activated T cells
UCD-T2DM rats	type 2 diabetic rat model expressing only wild-type rat amylin

rat amylin, which does not form amyloids (UCD-T2DM rats).[32] UCD-T2DM rats were obtained by breading obese SD rats with Zucker Diabetic Lean rats that lack the leptin receptor defect and have inherent ß-cell defects.[32] UCD-T2DM rats exhibit insulin resistance before the onset of diabetes,[32] similar to HIP rats[30] and humans.[1] In the present study, we used age-matched HIP (n=17) and UCD-T2DM (n=19) rats in the prediabetic state, that is, nonfasting blood glucose level in the 150 to 200 mg/dL range.[33] Wild-type littermates (n=16) served as nondiabetic controls for HIP rats. Age-matched SD rats (n=13, Charles Rivers Laboratory) were controls for UCD-T2DM rats.

Immunochemistry

Western blot analysis was performed on left ventricular homogenates, myocyte lysates, and blood serum. Immunohistochemistry was done on thin sections from paraffin blocks.

Insulin Signaling

Myocardial insulin responsiveness was determined by measuring the phosphorylation level of protein kinase B (Akt) and glycogen synthase kinase 3β (GSK3β) in hearts from rats injected (IP) with insulin (10 mU/g body weight) and euthanized 10 minutes after injection.

Cardiac Myocyte Isolation and Ca^{2+} Measurements

Rat ventricular myocytes were isolated by perfusion with 1 mg/mL collagenase on a Langendorff apparatus as previously reported.[34] Intracellular Ca^{2+} level ($[Ca^{2+}]_i$) was measured with Fura2 or Fluo4.

Activation of Ca^{2+}-Dependent Hypertrophic Pathways

Activation of Ca^{2+}/calmodulin-dependent protein kinase II (CaMKII)-histone deacetylase (HDAC) and calcineurin-nuclear factor of activated T cells (NFAT) hypertrophic pathways was examined by determining the nuclear versus cytosolic localization of HDAC4 and NFATc4 in cardiac myocytes using immunofluorescence.

In Vivo Echocardiography and Hemodynamics

M-mode echocardiography and hemodynamic measurements were performed as described before.[35]

Electron Microscopy

Aliquots of human/rat amylin aggregation reaction were imaged by a Philips CM 12 electron microscope, as previously described.[36]

Statistical Analysis

Data are expressed as mean±SEM. Statistical discriminations were performed using 2-tailed unpaired Student t test, with $P<0.05$
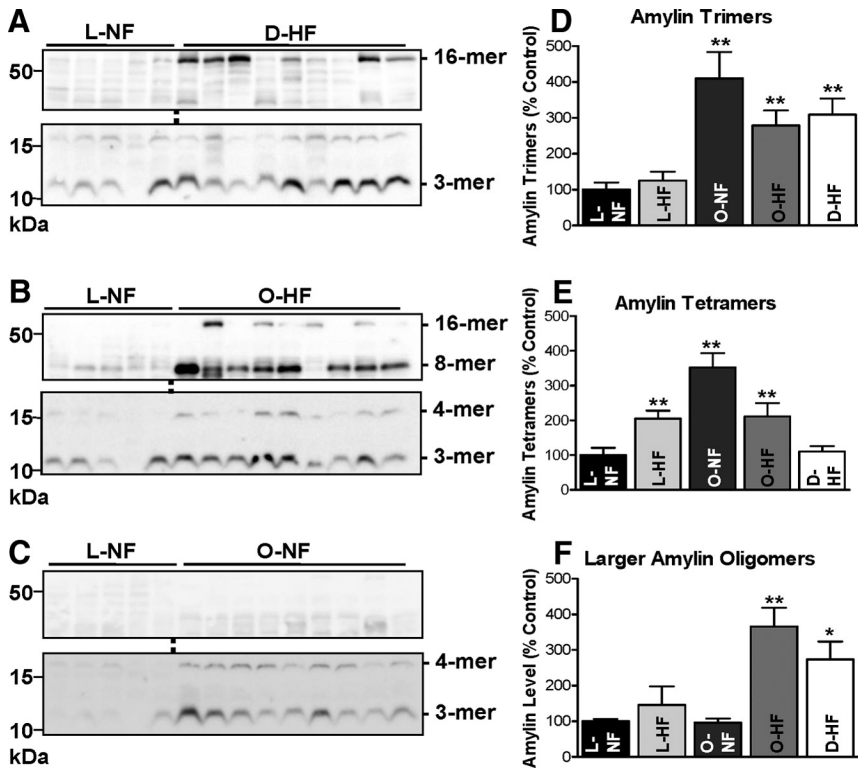
Figure 1. A through C, Amylin oligomer size distribution in failing (HF) and non-failing (NF) hearts from diabetic (D) and overweight/obese (O) patients versus lean (L) controls. Representative (of ≥4 experiments) Western blots with anti-amylin antibody of left ventricle protein homogenates from hearts in the D-HF (**A**), O-HF (**B**), and O-NF (**C**) groups. In each case, comparisons are made with hearts from the L-NF group. Specific molecular weight bands correspond to amylin trimers (12 kDa), tetramers (16 kDa), and 2 larger molecular weight structures at ≈32 kDa (octamers) and ≈64 kDa (16-mers). **D** through **F**, Intensity signal analysis of the 12, 16, and the integrated 32- to 64-kDa bands. Heart samples in the D-HF (n=25), O-HF (n=8), and O-NF (n=8) groups contain markedly higher amylin oligomer levels than the controls L-NF (n=5) and L-HF (n=7). Large-size amylin octamers and 16-mers are abundantly present only in the failing heart O-HF and D-HF groups. *$P<0.05$; **$P<0.01$.

considered significant. One-way ANOVA with the Dunnett post hoc test was used when comparing multiple groups.

Results

Patients With Obesity and Type 2 Diabetes Present Cardiac Amylin Accumulation

We examined left ventricular tissue from 53 human hearts divided in 5 pathologically distinct groups (Online Table I). These included failing hearts from patients with type 2 diabetes (n=25) and obese patients that developed overt type 2 diabetes within 1 year after transplantation (n=8). These hearts were expected to show significant amylin accumulation. To uncover the early stage of amylin buildup in the heart, a third group included nonfailing hearts from overweight/obese humans (n=8). Last, nonfailing hearts from lean, healthy patients (n=5) and failing hearts from lean patients without diabetes (n=7), which should not accumulate amylin, served as negative controls.

To assess the level and size distribution of cardiac amylin aggregates, we performed Western blots with an anti-amylin antibody on left ventricular protein homogenates. We found molecular weight bands corresponding to amylin trimers (12 kDa), tetramers (16 kDa), and 2 additional larger molecular weight structures at ≈32 kDa (octamers) and ≈64 kDa (16-mers) (Figure 1A through 1C). Negative controls showed that these bands are specific (Online Figure I). Intensity signal analysis (Figure 1D through 1F) indicated that amylin oligomer accumulation is markedly larger in failing hearts from patients with type 2 diabetes and overweight/obesity

than in normal hearts and failing hearts from patients without diabetes (controls). Intriguingly, large amylin oligomers, (32≥kDa) are abundant in failing hearts from diabetic and obese patients (Figure 1A, 1B, and 1F) but not in nonfailing hearts from overweight/obese individuals (Figure 1C and 1F). Smaller amylin oligomers were already elevated in nonfailing hearts from overweight/obese patients (Figure 1C through 1E), indicating an early stage of cardiac amylin accumulation. The results are consistent with the idea that accumulation of large amylin oligomers can induce deleterious cardiac effects. Amylin tetramers are also present in failing hearts from nondiabetic patients (Figure 1E), which might indicate undiagnosed insulin resistance in those patients (as commonly seen in aging).

Immunohistochemistry with an anti-amylin antibody shows large amylin deposits in failing hearts from type 2 diabetic patients (Figure 2A through 2D), similar to those found in the pancreas of type 2 diabetic patients (Figure 2F). Amylin plaques (Figure 2A, 2C, and 2D) and fibrillar tangles (Figure 2B) are scattered through the entire heart. Amylin deposits are often seen at sites with myocyte multinucleation, variation in nuclear size and infiltrating cells, which usually occur with fibrotic and infiltrative diseases. In contrast, sections from normal hearts (Figure 2E) do not show amylin deposition and structural abnormalities. To quantify the extent of amylin deposition in large plaques and fibrils, pellets from heart protein homogenates were treated with formic acid and guanidine hydrochloride to partially break down the amylin oligomers. Dot blots showed significantly increased amylin levels (Online Figure II), indicating that fragmenting of large amylin aggregates enhanced detection
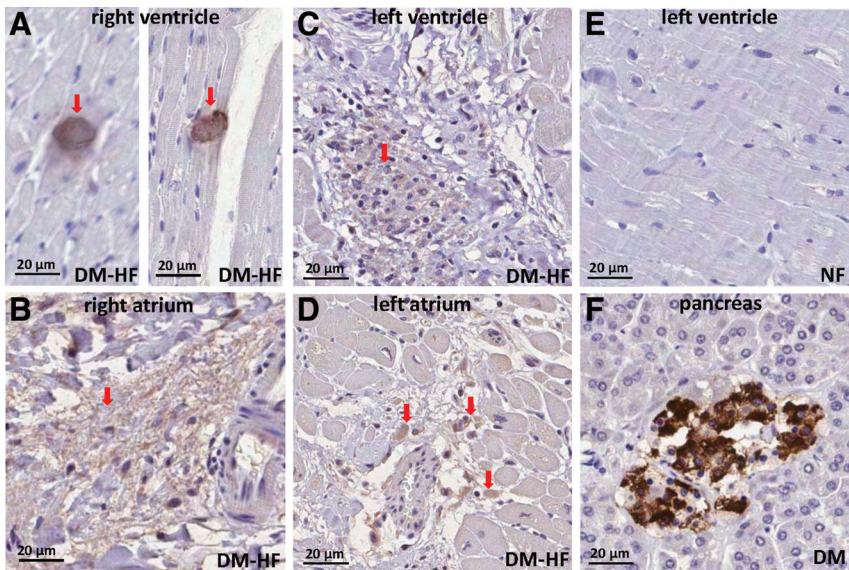
Figure 2. Amylin deposition in failing diabetic hearts demonstrated by immunohistochemistry with an anti-amylin antibody on thin heart sections. Amylin plaques (**A**, **C**, and **D**, **arrows**) and tangles (**B**, **arrow**) are scattered through the entire heart. **E**, Left ventricle section from a nonfailing heart; no amylin deposits are revealed. **F**, Positive control for amylin deposition in a pancreas from a diabetic patient.

by the anti-amylin antibody. This also implies that blots exhibiting higher order oligomers (Figure 1) probably underestimate the amount of amylin in these aggregates.

Human But Not Rat Amylin Alters Cardiac Myocyte Structure and Function Ex Vivo

Amylin oligomers elevate $[Ca^{2+}]_i$ in pancreatic β-cells leading to cellular dysfunction and apoptosis.[37] Similarly, β-amyloid oligomers induce neuron dysfunction and death in Alzheimer disease through a mechanism involving increased $[Ca^{2+}]_i$.[20,24,25] Thus, we examined Ca^{2+} cycling in cardiac myocytes incubated with exogenous amylin oligomers. Rat cardiac myocytes were incubated for ≈ 2 hours with 5 or 50 μmol/L exogenous human (amyloidogenic) or rat (nonamyloidogenic) amylin. Electron microscopy showed that at 50 μmol/L and 2 hours of incubation time, human but not rat amylin forms oligomers (Online Figure III); 50 μmol/L human amylin significantly increased Ca^{2+} transient amplitude (Figure 3A and 3C). In contrast, same concentration of nonamyloidogenic rat amylin had only a modest, not significant effect (Figure 3B). Incubation with either human or rat amylin (50 μmol/L) did not alter Ca^{2+} transient decay and diastolic $[Ca^{2+}]_i$ (Online Figure IV). This suggests that amylin does not directly affect SERCA function.

To determine if amylin oligomers elevate $[Ca^{2+}]_i$ by increasing sarcolemmal Ca^{2+} permeability, we measured the effect of human amylin oligomers on the passive sarcolemmal Ca^{2+} leak. We measured the initial rate of $[Ca^{2+}]_i$ decline on reducing $[Ca^{2+}]_0$ from 1 mmol/L to 0, with the SR, Na^+/Ca^{2+} exchanger and sarcolemmal Ca^{2+}-ATPase blocked (Figure 3D). Trans-sarcolemmal Ca^{2+} leak was significantly larger in myocytes preincubated with 50 μmol/L human amylin versus control (Figure 3E), suggesting alteration of sarcolemmal processes. Incubation of isolated myocytes with fluorescent human amylin showed that amylin attaches to the sarcolemma (Online Figure V, B). Human amylin monomers, dimers, and trimers were present in lysates

of myocytes preincubated with 50 μmol/L human amylin (Online Figure V, A), in agreement with human amylin attachment to sarcolemma. Thus, amylin oligomers attach to sarcolemma and raise cellular Ca^{2+} load in cardiac myocytes, an effect generated also in neurons[25] and pancreatic β-cells.[26,37]

Cardiac Amylin Accumulation Alters Ca^{2+} Cycling in HIP Rats

To test whether in vivo cardiac accumulation of human amylin affects Ca^{2+} cycling, we used prediabetic HIP rats. Age-matched, prediabetic UCD-T2DM rats expressing only the native, nonamyloidogenic rat amylin were used as negative control. Using prediabetic rats has the advantage that one can dissociate the effect of cardiac amylin accumulation from other confounding factors that affect cardiac Ca^{2+} cycling during late diabetes.[7,38,39] Immunohistochemistry (Figure 4A) and dot blots (Figure 4B) with an anti-amylin antibody that recognizes both human and rat amylin (the latter with higher avidity) show that amylin significantly accumulates only in HIP rat hearts. Western blots on left ventricular homogenates and cardiac myocyte lysates from HIP rats (Figure 4C) show amylin multimers similar to those detected in humans (Figure 1A through 1C) in all groups. These data indicate that amylin oligomer accumulation in HIP rat hearts starts from prediabetes. The presence of amylin oligomers in cardiac myocyte lysates suggests that they attach to sarcolemma and/or enter the myocytes.

To test whether cardiac amylin accumulation affects myocardial insulin responsiveness, we compared the activation status of Akt and GSK-3β, key components of the cardiac insulin signaling pathway, in HIP, littermate control, and UCD-T2DM rats. For this test, HIP and UCD-T2DM rats were matched for age and nonfasting blood glucose level (Figure 4D). The ratio between basal levels of phosphorylated Akt and total Akt is not statistically different among the three groups (Figure 4E and 4F). Insulin stimulation significantly increased the phosphorylation of Akt in all rats and no
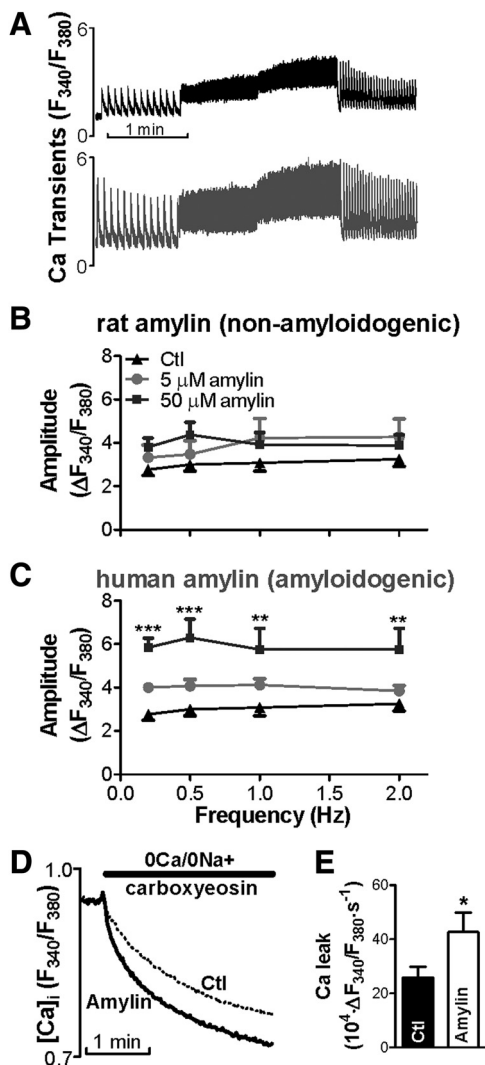
Figure 3. Exogenous human amylin oligomers increase Ca²⁺ transient amplitude in isolated rat cardiac myocytes. A, Representative Ca²⁺ transient measurements in a control (**top panel**) cell and a myocyte preincubated with 50 μmol/L human amylin (**bottom panel**). **B** and **C**, Effect of 5 and 50 μmol/L of rat (**B**) and human (**C**) amylin on Ca²⁺ transient amplitude. Oligomerization of human amylin resulted in a marked Ca²⁺ transient increase. **D**, Passive sarcolemmal Ca²⁺ leak measurements as initial slope of $[Ca^{2+}]_i$ decline on reducing external $[Ca^{2+}]$ from 1 mmol/L to 0, with the SR, Na⁺/Ca²⁺ exchanger and sarcolemmal Ca²⁺-ATPase blocked by pretreatment with thapsigargin, 0 Na⁺/0 Ca²⁺ solution and 20 μmol/L carboxyeosin, respectively. **E**, Passive trans-sarcolemmal Ca²⁺ leak is significantly larger in myocytes pretreated with 50 μmol/L human amylin versus control. For each group, measurements were done on ≥6 myocytes from 3 different rats.

statistical difference was observed among HIP, UCD-T2DM, and control groups (Figure 4E and 4F). GSK-3β displays a similar response to stimulation by insulin (Online Figure VI).

Cardiac amylin accumulation in prediabetic HIP rats alters myocyte Ca²⁺ cycling (Figure 5). At low stimulation frequencies, Ca²⁺ transient amplitude is significantly larger (4.7±0.5 versus 3.5±0.3 at 0.5 Hz) in myocytes from prediabetic HIP rats versus control rats (Figure 5A and 5D). In contrast, cardiac myocytes from age-matched, prediabetic UCD-T2DM rats show no change in Ca²⁺ transient amplitude

(Figure 5G and Online Figure VII). Thus, cardiac amylin accumulation may be the cause for the larger Ca²⁺ transient amplitude in prediabetic HIP rats, in agreement with our results using exogenous human amylin oligomers (Figure 3). Different from littermate controls, the amplitude of Ca²⁺ transients in myocytes from prediabetic HIP rats decreases with increasing the stimulation frequency (negative staircase), so that at 2 Hz the amplitude is similar to that recorded in control rats (Figure 5B and 5D). This is probably due to deficiencies in Ca²⁺ reuptake into the SR. Indeed, Ca²⁺ transient decline, which is mostly due to SR Ca²⁺ reuptake via the SR Ca-ATPase (SERCA), is significantly slower in prediabetic HIP rats versus control (τ=0.71±0.07 versus 0.55±0.04 s at a stimulation rate of 0.5 Hz; Figure 5C and 5E). In contrast, Ca²⁺ transient decay remains unchanged in myocytes from age-matched, prediabetic UCD-T2DM rats (Figure 5H). Despite slower Ca²⁺ transient relaxation, the SR Ca²⁺ load, assessed as the amplitude of Ca²⁺ transient produced by 10 mmol/L caffeine, is similar in myocytes from control and prediabetic HIP rats paced at 2 Hz (ΔF/F₀=8.5±0.4 versus 8.6±0.5). However, the slower Ca²⁺ transient relaxation in prediabetic HIP rats results in elevated diastolic $[Ca^{2+}]_i$ at higher pacing rates (Figure 5B and 5F). Diastolic $[Ca^{2+}]_i$ is unaltered in prediabetic UCD-T2DM rats (Figure 5I). Similar to myocytes incubated with human amylin, the sarcolemmal Ca²⁺ leak was significantly larger in prediabetic HIP rats versus control (41.6±4.5 versus 29.2±2.4 $10^4 \cdot \Delta F_{340}/F_{380} \cdot s^{-1}$, $P<0.05$). We infer that amylin oligomers can acutely increase Ca²⁺ leak into myocytes, causing elevated diastolic $[Ca^{2+}]_i$ and Ca²⁺ transients, but that reduced SERCA function may be a longer-term effect, as in heart failure.

HDAC and NFAT Translocation in Prediabetic HIP Rats and Myocytes Incubated With Human Amylin

Larger Ca²⁺ transients and elevated diastolic $[Ca^{2+}]_i$ may activate Ca²⁺-dependent hypertrophic signaling, such as CaMKII-HDAC and calcineurin-NFAT pathways.[40,41] High $[Ca^{2+}]_i$ activates CaMKII, which phosphorylates HDAC. Normally, HDAC represses transcriptional activation. However, HDAC phosphorylation causes its export from the nucleus, which activates hypertrophic gene expression. In the calcineurin-NFAT pathway, on activation by Ca²⁺/calmodulin, calcineurin dephosphorylates NFAT, causing NFAT import into the nucleus, which activates hypertrophic gene transcription. Using immunofluorescence, we found lower nuclear-to-cytosolic ratio of HDAC4 in myocytes from prediabetic HIP versus littermate controls (Figure 6A and 6C), indicating nuclear HDAC export. In contrast, the nuclear-to-cytosolic ratio of NFATc4 is elevated in prediabetic HIP rats (Figure 6B and 6D), suggesting the nuclear import of NFAT. Thus, both CaMKII-HDAC and calcineurin-NFAT hypertrophic pathways may be activated in prediabetic HIP rats.

NFATc4 was also translocated to the nucleus in control rat myocytes incubated with 50 μmol/L human amylin for 2 hours (Online Figure VIII). At this concentration, human amylin forms oligomers and fibrils and elevates Ca²⁺ tran-
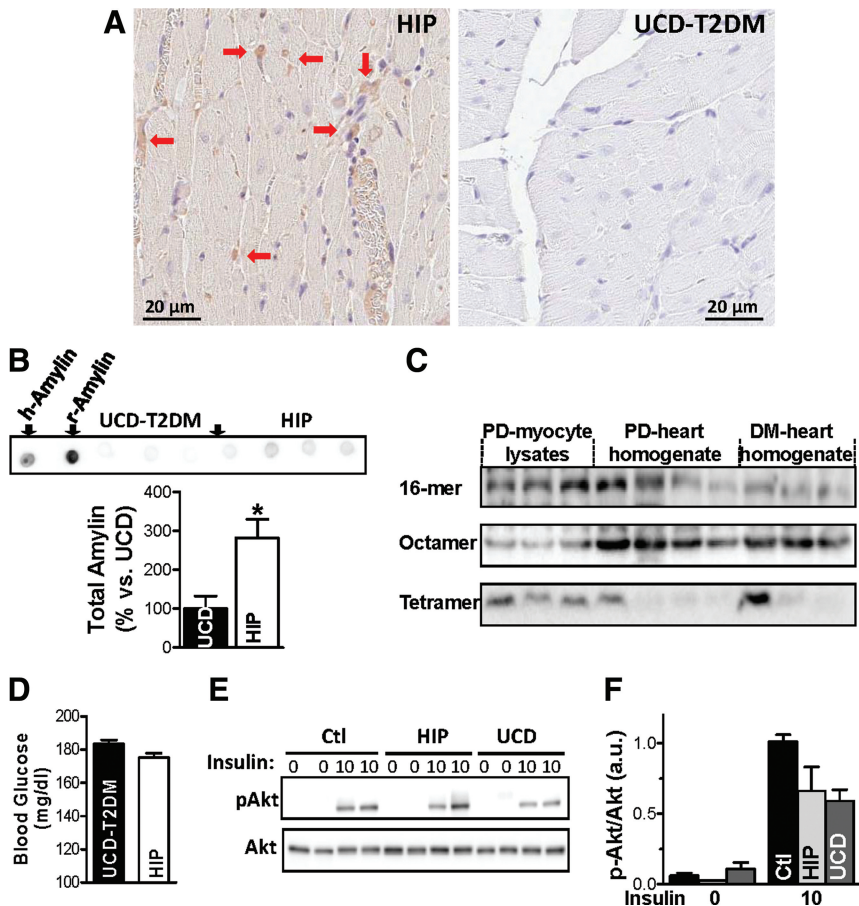
Figure 4. **A,** Immunohistochemistry with an anti-amylin antibody on thin heart sections demonstrating amylin deposition in cardiac tissues from prediabetic HIP but not UCD-T2DM rats (×20). **B,** Dot blots with the anti-amylin antibody comparing total amylin level in HIP versus UCD-T2DM rats. The first 2 dots on the left show positive controls using 5 ng of recombinant human (h-Amylin) and rat (r-Amylin) amylin. The antibody binds r-Amylin with significantly higher affinity than h-amylin; **Bottom panel** shows the average signal intensity in hearts from prediabetic HIP versus UCD-T2DM rats. The experiment was performed in triplicate. **C,** Representative Western blot with anti-amylin primary antibody on ventricular myocyte lysates from prediabetic HIP rats, and left ventricle protein homogenates from prediabetic (PD) and diabetic (DM) HIP rats. **D,** Blood glucose levels in age-matched prediabetic HIP rats (n=14) and UCD-T2DM rats (n=16). **E** and **F,** Akt phosphorylation in hearts from prediabetic HIP and UCD-T2DM rats and littermate controls under basal conditions (0 insulin) and after stimulation with insulin (10 mU/g body weight). Representative example (**E**) and mean values for the ratio between phosphorylated and total Akt (**F**); n=3 rats for each group.

sients, as discussed in above. The distribution of HDAC4 was not altered by this acute amylin exposure (Online Figure VIII). We conclude that Ca^{2+}-dependent nuclear signaling initiated by amylin oligomers is capable of inducing hypertrophic transcriptional effects.

Cardiac Amylin Accumulation Accelerates Cardiac Hypertrophy and Remodeling

Elevated natriuretic peptide levels are thought to reflect cardiac dysfunction and have been used as a "biomarker" of cardiac hypertrophy.[42,43] We found that the level of brain natriuretic peptide (BNP) is elevated (by 100±30%) in hearts from prediabetic HIP rats versus littermate controls and further increases with diabetes development (Figure 6E). This suggests hormonal alterations specific to the onset of cardiac hypertrophy in HIP rats. In contrast, the BNP level is not altered in prediabetic UCD-T2DM rats and only increases after the full development of diabetes (Online Figure IX, A). Of note, a previous study found that external human amylin induces hypertrophy in isolated cardiac myocytes.[44] However, the heart weight/body weight ratio in prediabetic HIP rats (2.72±0.22 g) versus control rats (2.71±0.2 g) did not change, showing the lack of overt cardiac hypertrophy in this early disease state.

Activation of Ca^{2+}-dependent transcriptional pathways may also alter the transcription of key Ca^{2+} transport and regulatory proteins, which cause further alterations in Ca^{2+}

cycling. Thus, we measured the protein expression of SERCA, phospholamban (the endogenous SERCA inhibitor), and Na^+/Ca^{2+} exchanger, the main Ca^{2+} extrusion pathway in HIP rats (Figure 6F). We found that SERCA expression is reduced by 20% and 30% in prediabetic and diabetic HIP rats, respectively (Figure 6F). In contrast, SERCA expression was unchanged in prediabetic UCD-T2DM rats (Online Figure IX, B). Protein expressions of phospholamban and Na^+/Ca^{2+} exchanger are unaltered in prediabetic HIP rats (Figure 6F).

Prediabetic HIP Rats Show Diastolic Dysfunction

To determine how amylin accumulation affects cardiac function, we performed in vivo echocardiography and hemodynamic measurements on prediabetic HIP rats (Table). We found significantly slower relaxation (reduced $-dP/dt_{min}$ values) in prediabetic HIP rats versus control. This suggests that cardiac amylin oligomer accumulation may accelerate the occurrence of heart dysfunction, particularly diastolic dysfunction, a typical sign of diabetic cardiomyopathy.[2–10,38,39] Furthermore, the left ventricular end diastolic volume is increased in prediabetic HIP rats, which, combined with the unchanged fractional shortening, suggests dilation of the heart (Table).

Discussion

We found significant accumulation of large amylin oligomers (>octamers, Figure 1A, 1B, and 1F), fibrillar tangles (Figure
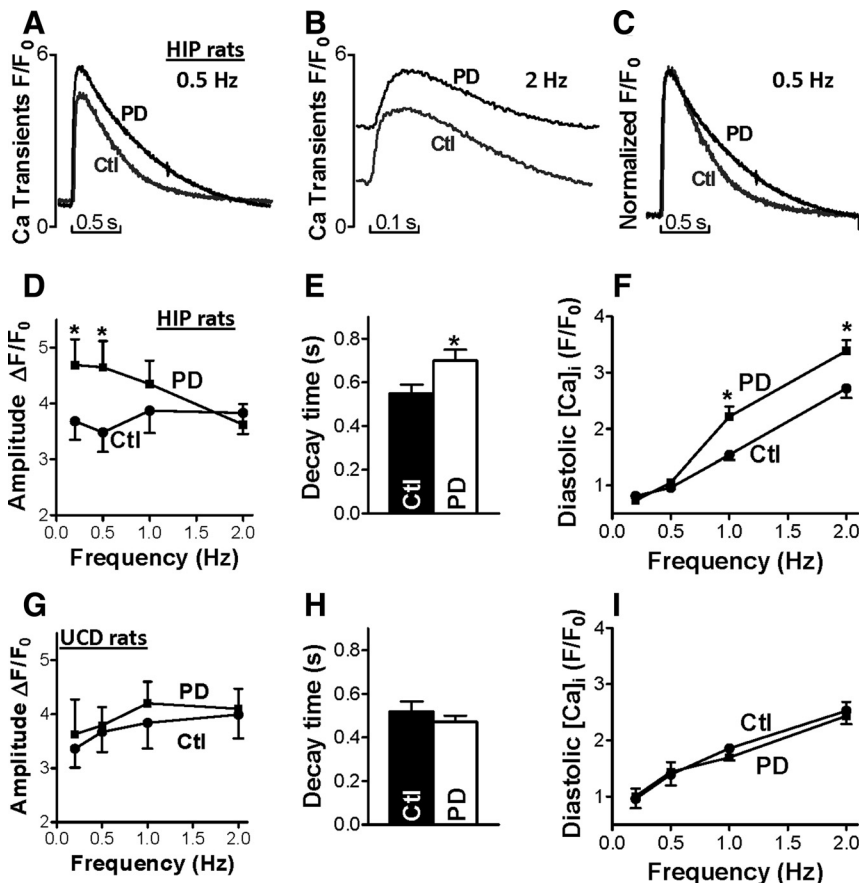
**Figure 5. Altered Ca^{2+} cycling in cardiac myocytes from prediabetic HIP but not prediabetic UCD-T2DM rats.** Representative Ca^{2+} transients in myocytes from control (Ctl) and prediabetic (PD) HIP rats paced at 0.5 Hz (**A**) and 2 Hz (**B**). **C**, Normalized Ca^{2+} transients in myocytes from control and prediabetic HIP rats (0.5 Hz) indicate slower Ca^{2+} transient relaxation in prediabetic HIP rats versus control. **D**, Mean amplitude of Ca^{2+} transients recorded in cardiac myocytes from control rats (20 myocytes, 4 rats) and prediabetic HIP rats (18 cells, 4 rats) paced at 0.2, 0.5, 1, and 2 Hz. At 0.2 and 0.5 Hz, Ca^{2+} transient amplitude is significantly larger in myocytes from prediabetic HIP rats versus control. This difference disappears at higher stimulation frequencies. **E**, Ca^{2+} transient decay time in cardiac myocytes from control and prediabetic HIP rats paced at 0.5 Hz. **F**, Diastolic [Ca^{2+}]$_i$ in cardiac myocytes from control rats and prediabetic HIP rats paced at 0.2, 0.5, 1, and 2 Hz. At higher frequencies, diastolic [Ca^{2+}]$_i$ is significantly higher in myocytes from prediabetic HIP versus control rats. **G**, Mean amplitude of Ca^{2+} transients in myocytes from control rats (22 myocytes, 6 rats) and prediabetic UCD-T2DM rats (21 cells, 4 rats) paced at 0.2, 0.5, 1, and 2 Hz. **H**, Ca transient decay time in myocytes from control and prediabetic UCD-T2DM rats paced at 0.5 Hz. **I**, Diastolic [Ca^{2+}]$_i$ in myocytes from control and prediabetic UCD-T2DM rats paced at 0.2, 0.5, 1, and 2 Hz. *$P<0.05$.

2B), and plaques (Figure 2A, 2C, and 2D) in failing hearts from patients with obesity and type 2 diabetes, but not in normal hearts and failing hearts from lean humans without diabetes (Figure 1C and 1F). Small amylin aggregates are even elevated in nonfailing hearts from overweight/ obese patients (Figure 1C through 1E), suggesting that cardiac amylin buildup starts in the early state of insulin resistance/ prediabetes. HIP rats, which express human amylin in the pancreas, accumulate amylin oligomers in the heart (Figure 4A through 4C) starting also in prediabetes. In prediabetic HIP rats, the interaction of amylin oligomers with cardiac myocytes results in larger sarcolemmal Ca^{2+} leak and Ca^{2+} transients (Figure 5A and 5D) leading to activation of Ca^{2+}-mediated hypertrophic pathways (Figure 6A through 6D), pathological heart remodeling (Figure 6E and 6F), and diastolic dysfunction (Figure 5E and 5F and the Table). In contrast, UCD-T2DM rats, which are matched for age, blood glucose level (Figure 4D), and myocardial insulin responsiveness (Figure 4E and 4F) but lack amylin deposition (Figure 4A and 4B), have normal cardiac structure (Figure 4A and 4B) and function (Figure 5G through 5I). These results suggest that cardiac dysfunction in HIP rats is most likely an amylin-mediated effect. Hence, hyperamylinemia and consequent amylin deposition, a toxic effect generally assumed to contribute to pancreatic β-cell dysfunction and development of type 2 diabetes,[13,14,31,45,46] may also be causally implicated in cardiac dysfunction.

Pathologically Important Form of Amylin

Conditions underlying amylin oligomerization[13–15,45,46] and proteotoxicity[21,22] are complex and only poorly understood. Amyloidogenicity of human amylin promotes the attachment to the sarcolemma (Online Figure V, B) and oligomer formation, 2 apparently independent processes. Small oligomers develop rapidly at the sarcolemma, for example, in only 1–2 hours (Online Figure V), which correlates with an increase in sarcolemmal permeability to Ca^{2+} (Figure 3D and 3E) and elevated Ca^{2+} transients (Figure 3A and 3C), with consequent activation of Ca^{2+}-mediated hypertrophic pathways (Online Figure VIII). In contrast, rat amylin, a nonamyloidogenic isoform of amylin[29] (Online Figure III), does not affect Ca^{2+} cycling when incubated with cardiac myocytes (Figure 3B). These results suggest that the oligomers may be the pathologically important forms of amylin. Amylin oligomerization at the sarcolemma may act as seeds for further amyloid growth. Fibril growth at the membrane amplifies structural alteration of the membrane[22] and Ca^{2+} dysregulation, aggravating the deleterious effects in the heart. This might be the case for the large amylin oligomers in the 32- to 64-kDa size range that are abundant in failing hearts from diabetic and obese patients (Figure 1A, 1B, and 1F) and in HIP rat hearts (Figure 4C).

There is increasing support for the toxic oligomer hypothesis in amyloid-related diseases,[20–28] including cardiomyopathies caused by other amyloidogenic proteins that infiltrate the heart, for example, transthyretin, immunoglobulin light
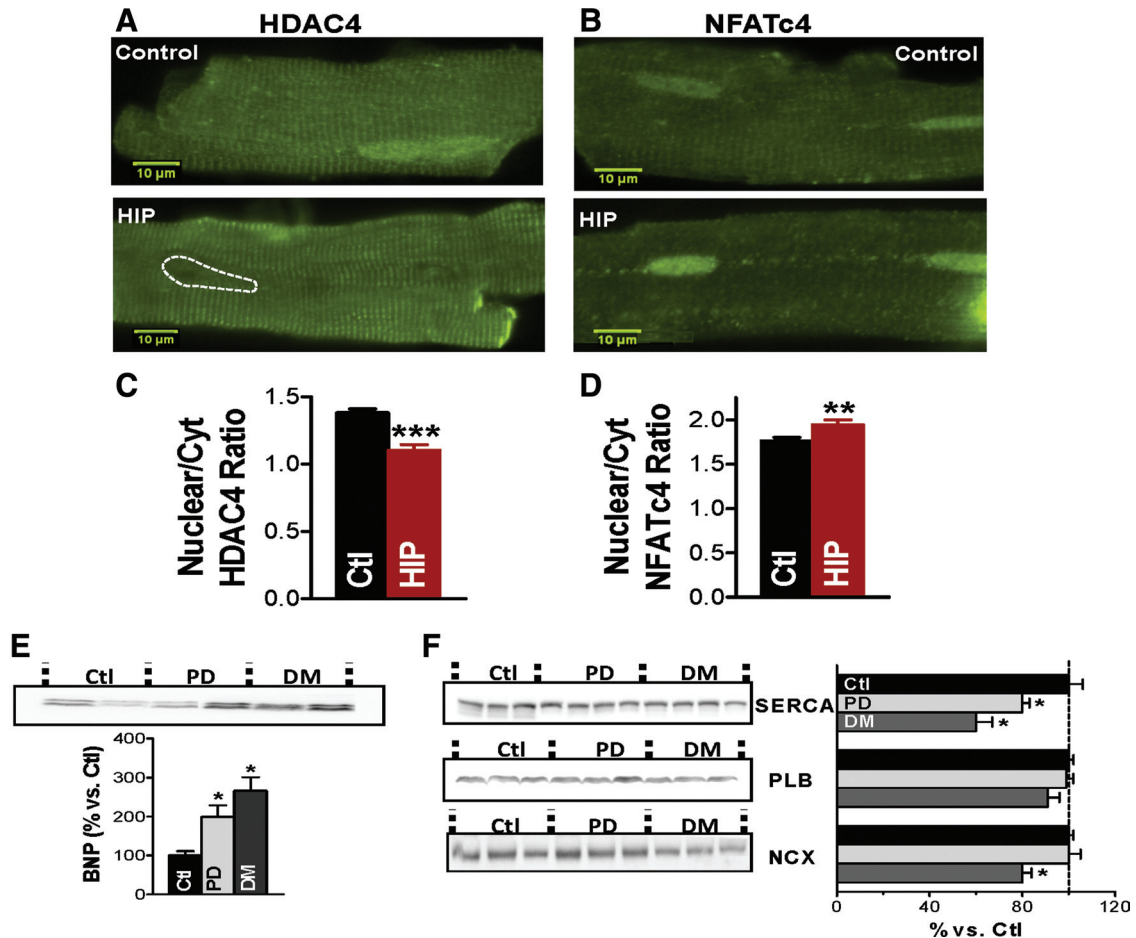
Figure 6. HDAC4 nuclear export, NFATc4 nuclear import , reduced SERCA and increased BNP in hearts from prediabetic HIP rats. A and **B**, Representative immunofluorescence images showing the distribution of HDAC4 and, respectively, NFATc4 in myocytes from prediabetic HIP rats and age-matched WT rats. **C** and **D**, The nuclear-to-cytosolic ratio of HDAC4 (**C**) and NFATc4 (**D**) demonstrates the nuclear export of HDAC4 and nuclear import of NFATc4 in prediabetic HIP rats. Experiments were done on more than 15 cells from 3 rats for both groups. **E**, Increased expression of the hypertrophic marker BNP in hearts from prediabetic (PD) and diabetic (DM) HIP rats. **F**, Alterations in the protein expression of SERCA, phospholamban and Na/Ca exchanger in hearts from prediabetic and diabetic HIP rats versus control, nondiabetic rats (Ctl). Ctl, 5 hearts; PD, 5 hearts, DM, 5 hearts.

chain, and serum amyloid.[47] Data[48,49] suggest that the infiltration of amyloidogenic proteins in the heart may induce cardiotoxicity even before amyloid fibril formation. Moreover, intracellular accumulation of amyloid oligomers, such as those formed by polyglutamine[27] or presenilin,[28] induced cytotoxicity and heart failure in mice. Presenilin oligomers coimmunoprecipitated with SERCA and altered Ca^{2+} han-

dling.[28] Our data from human and HIP rat hearts suggest that amylin oligomer accumulation in the heart, which is an outside-inside cardiac event, is cardiotoxic and may represent an early pathogenic mechanism linking type 2 diabetes with cardiac dysfunction.

## Cardiac Amylin Accumulation and Altered Myocyte Ca^{2+} Cycling

Our data show that the primary effect of cardiac amylin oligomer accumulation is an increase in myocyte Ca^{2+} and Ca^{2+} transients (schematic in Figure 7). This effect was observed both in cardiac myocytes exposed acutely to human amylin and in prediabetic HIP rats, which accumulate amylin oligomers in the heart, but not in prediabetic UCD-T2DM rats that express only nonamyloidogenic rat amylin and thus lack cardiac oligomeric amylin accumulation. Such an effect agrees well with previous data showing that the toxicity associated with amyloidogenic proteins is mediated by an initial increase in $[Ca^{2+}]_i$.[20,25,37] Whereas the mechanisms underlying the increase of $[Ca^{2+}]_i$ are not fully elucidated, our data suggest that an augmented passive trans-

Table. Echo and Hemodynamic Parameters in Prediabetic HIP Rats (n=6) Versus Control (n=10)

	Control	HIP
Heart rate, bpm	208±14	231±17
Fractional shortening, %	66.7±3.4	57.8±2.8
LVEDD, mm	6.4±0.3	7.2±0.2*
dP/dt$_{max}$, mm Hg/s	7277±247	6597±672
−dP/dt$_{min}$, mm Hg/s	6237±411	4822±344*
LV$_{max}$ systolic pressure, mm Hg	107±2	99±3*
LV end-diastolic pressure, mm Hg	6.8±0.8	5.8±1.4

LVEDD indicates left ventricular end-diastolic diameter.
*$P<0.05$.
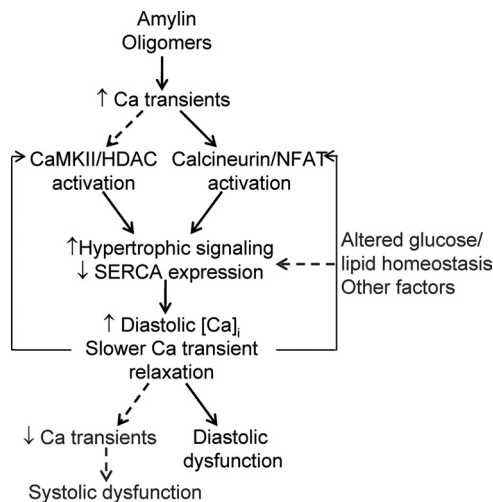
Figure 7. Proposed mechanism for amylin oligomer-induced cardiac dysfunction. Amylin oligomers elevate Ca^{2+} transients, which results in activation of Ca^{2+}-dependent CaMKII-HDAC and calcineurin-NFAT transcriptional regulation/hypertrophic pathways. This may reduce SERCA expression, which further alters myocyte Ca^{2+} cycling by impairing Ca^{2+} transient relaxation leading to higher diastolic $[Ca^{2+}]_i$. Impaired Ca^{2+} transient relaxation and elevated diastolic $[Ca^{2+}]_i$ may further activate the Ca^{2+}-dependent transcriptional regulation/hypertrophic pathways (positive feedback) and cause diastolic dysfunction in HIP rats. With the advancement of the disease, reduced SERCA function may cause SR unloading, consequent reduction in Ca^{2+} transient amplitude, and systolic dysfunction.

sarcolemmal Ca^{2+} flux is partly responsible. Amylin oligomers may also modulate the function of Ca^{2+} channels, as proposed in the pathology of Alzheimer disease.[20,50] Elevated $[Ca^{2+}]_i$ is involved in transcriptional regulation and hypertrophic signaling in the heart.[40,41] Both CaMKII-HDAC and calcineurin-NFAT hypertrophic pathways are activated in cardiac myocytes from prediabetic HIP rats (Figure 6A through 6D). Moreover, the calcineurin-NFAT pathway can be activated even by acute exposure of isolated myocytes to human amylin oligomers (Online Figure VIII). These data implicate the amylin oligomers as a trigger of hypertrophic and remodeling maladaptive changes in the heart (Figure 7). Prediabetic HIP rats show SERCA downregulation (Figure 6F), a common occurrence in diabetic cardiomyopathy,[51] and increased level of the prohypertrophic hormone BNP (Figure 6E). SERCA downregulation causes further alterations in cardiac myocyte Ca^{2+} cycling by impairing Ca^{2+} transient relaxation, which leads to negative force-frequency relationship (Figure 5D) and elevated diastolic $[Ca^{2+}]_i$ (Figure 5F). Slower Ca^{2+} transient relaxation and elevated diastolic $[Ca^{2+}]_i$ may further activate the CaMKII-HDAC and calcineurin-NFAT transcriptional regulation/hypertrophic pathways and thus aggravate the cardiac hypertrophy and remodeling (Figure 7). Furthermore, impaired Ca^{2+} transient relaxation and elevated diastolic $[Ca^{2+}]_i$ cause diastolic dysfunction in prediabetic HIP rats (Table). None of these alterations were present in prediabetic UCD-T2DM rats. Alterations in function and/or expression of proteins involved in cardiac Ca^{2+} cycling, including SERCA, and diastolic dysfunction have been reported in other rodent models of type 2 diabetes, but only after the onset of full-blown type 2

diabetes.[7,38,39] Thus, our data indicate that cardiac amylin oligomer accumulation accelerates the occurrence of cardiac dysfunction and remodeling in diabetes.

Amylin Oligomer–Induced Cardiac Phenotype
At the whole-heart level, HIP rats show pathological signs of an infiltrative disease[52] (Table). This is characterized by diastolic dysfunction (significantly reduced $-dP/dt_{min}$) and unchanged fractional shortening, which is one type of diastolic heart failure.[52] Diastolic heart failure often progresses to systolic failure. Hemodynamics and echocardiographic measurements in HIP rats show indeed significantly reduced maximum rate of pressure fall ($-dP/dt_{min}$), an index of diastolic dysfunction, along with unchanged fractional shortening (Table). The left ventricular maximum systolic pressure is also significantly reduced in HIP rats (Table). Hence, prediabetic HIP rats display cardiac changes resembling the cardiac infiltrative disease in humans.[52] Diastolic dysfunction is also important in the pathogenesis of diabetic cardiomyopathy.[2–10,38,39] The molecular mechanisms underlying diastolic dysfunction in diabetic patients are poorly understood.[2–10,38,39] Present data suggest that cardiac amylin oligomer accumulation is linked to Ca^{2+} dysregulation and pathological cardiac hypertrophy, which may accelerate the onset of diastolic dysfunction in diabetes.

The pathogenesis of diabetic cardiomyopathy is multifactorial and includes metabolic components[2–10,38,39] that have not been studied here. Additional work to address any potential influences of the amylin oligomers on key metabolic processes in the heart is needed.

In conclusion, our data show that patients with obesity and type 2 diabetes accumulate amylin oligomers in the heart and suggest that this accelerates the development of cardiac dysfunction. We propose that detection and disruption of cardiac amylin buildup may be a predictor of myocardial dysfunction and a novel therapeutic target in diabetic cardiomyopathy.

References

1. Biddinger SB, Kahn CR. From mice to men: insights into the insulin resistance syndromes. *Annu Rev Physiol*. 2006;68:123–158.
2. Lopaschuk GD, Ussher JR, Folmes CD, Jaswal JS, Stanley WC. Myocardial fatty acid metabolism in health and disease. *Physiol Rev*. 2010; 90:207–258.
3. Reaven GM. Relationships among insulin resistance, type 2 diabetes, essential hypertension, and cardiovascular disease: similarities and differences. *J Clin Hypertens*. 2011;13:238–243.
4. Battiprolu PK, Gillette TG, Wang ZV, Lavandero S, Hill JA. Diabetic cardiomyopathy: mechanisms and therapeutic targets. *Drug Discov Today Dis Mech*. 2010;7:e135–e143.
5. Guha A, Harmancey R, Taegtmeyer H. Nonischemic heart failure in diabetes mellitus. *Curr Opin Cardiol*. 2008;23:241–248.
6. Boudina S, Abel ED. Diabetic cardiomyopathy, causes and effects. *Rev Endocr Metab Disord*. 2010;11:31–39.
7. Lebeche D, Davidoff AJ, Hajjar RJ. Interplay between impaired calcium regulation and insulin signaling abnormalities in diabetic cardiomyopathy. *Nat Clin Pract Cardiovasc Med*. 2008;5:715–724.
8. Young LH. Diet-induced obesity obstructs insulin signaling in the heart. *Am J Physiol Heart Circ Physiol*. 2010;298:H306–H307.
9. Swan JW, Anker SD, Walton C, Godsland IF, Clark AL, Leyva F, Stevenson JC, Coats AJ. Insulin resistance in chronic heart failure: relation to severity and etiology of heart failure. *J Am Coll Cardiol*. 1997;30:527–532.
10. Ashrith G, Algahim MF, Taegtmeyer H. Insulin resistance: marker or mediator? *Am J Med*. 2009;122:e13–e15.
11. Utriainen T, Takala T, Luotolahti M, Ronnemaa T, Laine H, Ruotsalainen U, Haaparanta M, Nuutila P, Yki-Jarvien H. Insulin resistance characterizes glucose uptake in skeletal muscle but not in the heart in NIDDM. *Diabetologia*. 1998;41:555–559.
12. Jagasia D, Whiting JM, Concato J, Pfau S, McNulty PH. Effect of non-insulin-dependent diabetes mellitus on myocardial insulin responsiveness in patients with ischemic heart disease. *Circulation*. 2001;103: 1734–1739.
13. Johnson KH, O'Brien TD, Jordan K, Westermark P. Impaired glucose tolerance is associated with increased islet amyloid polypeptide (IAPP) immunoreactivity in pancreatic beta cells. *Am J Pathol*. 1989;135: 245–250.
14. Johnson KH, O'Brien TD, Betsholtz C, Westermark P. Islet amyloid, islet amyloid polypeptide and diabetes mellitus. *N Engl J Med*. 1989;321: 513–518.
15. Enoki S. Mitsukawa T, Takemura J, Nakazato M, Aburaya J, Toshimori H, Matsukara S. Plasma islet amyloid polypeptide levels in obesity, impaired glucose tolerance and non-insulin-dependent diabetes mellitus. *Diabetes Res Clin Pract*. 1992;15:97–102.
16. Gong W, Liu ZH, Zeng CH, Peng A, Chen HP, Zhou H, Li LS. Amylin deposition in the kidney of patients with diabetic nephropathy. *Kidney Int*. 2007;72:213–218.
17. Despa S, Chen L, Cummings B, Havel PJ, Margulies KB, Knowlton AA, Bers DM, Despa F. Cardiac consequences of increased amylin secretion in diabetics. *Circulation*. 2009;120:S457.
18. Despa S, Bers DM, Despa F. Accumulation of islet amyloid polypeptide (IAPP) oligomers in the heart in type 2 diabetes alters Ca cycling in myocytes. *Circulation*. 2010;122:A18345.
19. Colby DW, Prusiner SB. Prions. *Cold Spring Harb Perspect Biol*. 2011; 3:1–22.
20. Haass C, Selkoe DJ. Soluble protein oligomers in neurodegeneration: lessons from the Alzheimer's amyloid beta-peptide. *Nat Rev Mol Cell Biol*. 2007;8:101–112.
21. Janson J, Ashley RH, Harrison D, McIntyre S, Butler PC. The mechanism of islet amyloid polypeptide toxicity is membrane disruption by intermediate-sized toxic amyloid particles. *Diabetes*. 1999;48:491–498.
22. Engel MF, Khemtémourian L, Kleijer CC, Meeldijk HJ, Jacobs J, Verkleij AJ, de Kruijff B, Killian JA, Höppener JW. Membrane damage by human islet amyloid polypeptide through fibril growth at the membrane. *Proc Natl Acad Sci U S A*. 2008;105:6033–6038.
23. Anguiano M, Nowak RJ, Lansbury PT Jr. Protofibrillar islet amyloid polypeptide permeabilizes synthetic vesicles by a pore-like mechanism that may be relevant to type II diabetes. *Biochemistry*. 2002;41: 11338–11343.
24. Mattson MP, Goodman Y. Different amyloidogenic peptides share a similar mechanism of neurotoxicity involving reactive oxygen species and calcium. *Brain Res*. 1995;676:219–224.
25. Kawahara M, Kuroda Y, Arispe N, Rojas E. Alzheimer's beta-amyloid, human islet amylin, and prion protein fragment evoke intracellular free calcium elevations by a common mechanism in a hypothalamic GnRH neuronal cell line. *J Biol Chem*. 2000;275:14077–14083.
26. Casas S, Novials A, Reimann F, Gomis R, Gribble FM. Calcium elevation in mouse pancreatic beta cells evoked by extracellular human islet amyloid polypeptide involves activation of the mechanosensitive ion channel TRPV4. *Diabetologia*. 2008;51:2252–2262.
27. Pattison JS, Sanbe A, Maloyan A, Osinska H, Klevitsky R, Robbins J. Cardiomyocyte expression of a polyglutamine preamyloid oligomer causes heart failure. *Circulation*. 2008;117:2743–2751.
28. Gianni D, Li A, Tesco G, McKay KM, Moore J, Raygor K, Rota M, Gwathmey JK, Dec GW, Aretz T, Leri A, Semigran MJ, Anversa P, Macgillivray TE, Tanzi RE, del Monte F. Protein aggregates and novel presenilin gene variants in idiopathic dilated cardiomyopathy. *Circulation*. 2010;121: 1216–1226.
29. Westermark P, Engström U, Johnson KH, Westermark GT, Betsholtz C. Islet amyloid polypeptide: pinpointing amino acid residues linked to amyloid fibril formation. *Proc Natl Acad Sci U S A*. 1990;87: 5036–5040.
30. Matveyenko AV, Butler PC. Islet amyloid polypeptide (IAPP) transgenic rodents as models for type 2 diabetes. *ILAR J*. 2006;47:225–233.
31. Matveyenko AV, Butler PC. β-cell deficit due to increased apoptosis in the human islet amyloid polypeptide transgenic (HIP) rat recapitulates the metabolic defects present in type 2 diabetes. *Diabetes*. 2006;55: 2106–2114.
32. Cummings BP, Digitale EK, Stanhope KL, Graham JL, Baskin DG, Reed BJ, Sweet IR, Griffen SC, Havel PJ. Development and characterization of a novel rat model of type 2 diabetes mellitus: the UC Davis type 2 diabetes mellitus UCD-T2DM rat. *Am J Physiol Regul Integr Comp Physiol*. 2008;295:R1782–R1793.
33. http://www.nlm.nih.gov/medlineplus/ency/article/000313.htm.
34. Despa S, Bers DM. Functional analysis of Na/K-ATPase isoform distribution in rat ventricular myocytes. *Am J Physiol Cell Physiol*. 2007;293: C321–C327.
35. Lin L, Kim SC, Wang Y, Gupta S, Davis B, Simon SI, Torre-Amione G, Knowlton AA. HSP60 in heart failure: abnormal distribution and role in cardiac myocyte apoptosis. *Am J Physiol Heart Circ Physiol*. 2007;293: H2238–H2247.
36. Walton JH, Berry RS, Despa F, Amyloid oligomer formation probed by water proton magnetic resonance spectroscopy. *Biophys J*. 2010;100: 2302–2308.
37. Huang CJ, Gurlo T, Haataja L, Costes S, Daval M, Ryazantsev S, Wu X, Butler AE, Butler PC. Calcium-activated calpain-2 is a mediator of beta cell dysfunction and apoptosis in type 2 diabetes. *J Biol Chem*. 2010; 285:339–348.
38. Netticadan T, Temsah RM, Kent A, Elimban V, Dhalla NS. Depressed levels of Ca^{2+}-cycling proteins may underlie sarcoplasmic reticulum dysfunction in the diabetic heart. *Diabetes*. 2001;50:2133–2138.
39. Pereira L, Matthes J, Schuster I, Valdivia HH, Herzig S, Richard S, Gómez AM. Mechanisms of [Ca2+]i transient decrease in cardiomyopathy of db/db type 2 diabetic mice. *Diabetes*. 2006;55:608–615.
40. Bers DM. Calcium cycling and signaling in cardiac myocytes. *Annu Rev Physiol*. 2008;70:23–49.
41. Hill JA, Olson EN, Cardiac plasticity. *N Engl J Med*. 2008;358:1370–80.
42. Luchner A, Stevens TL, Borgeson DD, Redfield M, Wei CM, Porter JG, Burnett JC Jr. Differential atrial and ventricular expression of myocardial BNP during evolution of heart failure. *Am J Physiol Heart Circ Physiol*. 1998;274:H1684–H1689.
43. Ellmers LJ Knowles JW, Kim HS, Smithies O, Maeda N, Cameron VA. Ventricular expression of natriuretic peptides in Npr1(−/−) mice with cardiac hypertrophy and fibrosis. *Am J Physiol Heart Circ Physiol*. 2002;283:H707–H714.
44. Bell D, Schluter K-D, Zhou X-J, McDermott BJ, Piper HM. Hypertrophic effects of calcitonin gene related peptide (CGRP) and amylin on adult mammalian ventricular cardiomyocytes. *J Mol Cell Cardiol*. 1995;27: 2433–2443.
45. Ionescu-Tirgoviste C, Despa F. Biophysical alteration of the secretory track in β-cells due to molecular overcrowding: the relevance for diabetes. *Integr Biol (Camb)*. 2011;3:173–179.
46. Despa F. Endoplasmic reticulum overcrowding as a mechanism of beta-cell dysfunction in diabetes. *Biophys J*. 2010;98:1641–1648.
47. Falk RH, Dubrey SW. Amyloid heart disease. *Prog Cardiovasc Dis*. 2010;52:347–361.

48. Palladini G, Lavatelli F, Russo P, Perlini S, Perfetti V, Bosoni T, Obici L, Bradwell AR, D'Eril GM, Fogari R, Moratti R, Merlini G. Circulating amyloidogenic free light chains and serum N-terminal natriuretic peptide type B decrease simultaneously in association with improvement of survival in AL. *Blood*. 2006;107:3854–3858.
49. Liao R, Jain M, Teller P, Connors LH, Ngoy S, Skinner M, Falk RH, Apstein CS. Infusion of light chains from patients with cardiac amyloidosis causes diastolic dysfunction in isolated mouse hearts. *Circulation*. 2001;104:1594–1597.
50. Green KN, LaFerla FM. Linking calcium to abeta and Alzheimer's disease. *Neuron*. 2008;59:190–194.
51. Razeghi P, Young ME, Cockrill TC, Frazier OH, Taegtmeyer H. Down-regulation of myocardial myocyte enhancer factor 2C and myocyte enhancer factor 2C-regulated gene expression in diabetic patients with nonischemic heart failure. *Circulation*. 2002;106:407–411.
52. Seward JB, Casaclang-Verzosa G. Infiltrative cardiovascular diseases: cardiomyopathies that look alike, *J Am Coll Cardiol*. 2010;55:1769–1779.

Novelty and Significance

What Is Known?

- Patients with obesity and insulin resistance have elevated circulating levels of amylin, an amyloidogenic hormone coexpressed and cosecreted with insulin by pancreatic β-cells.
- At increased concentrations, amylin readily form amyloids, which are cytotoxic and contribute to the development of type 2 diabetes.
- The most toxic species of amylin amyloids are the soluble oligomers, which attach to cellular membranes causing Ca^{2+} dyshomeostasis, cell dysfunction, and apoptosis.

What New Information Does This Article Contribute?

- Amylin oligomers accumulate in the heart and are associated with cardiac failure in patients with obesity and type 2 diabetes.
- Amylin oligomer buildup in the heart of rats transgenic for human amylin is linked to myocyte Ca^{2+} dysregulation, pathological cardiac hypertrophy and remodeling, and diastolic dysfunction.
- Cardiac amylin accumulation accelerates the onset of diabetic cardiomyopathy.

Obesity and insulin resistance increase the risk for both type 2 diabetes and cardiac disease, but the underlying mechanisms remain poorly understood. In addition to hyperglycemia and dyslipidemia, patients with obesity and insulin resistance present also hyperinsulinemia and hyperamylinemia. Whereas the hyperinsulinemic response prevents a large fraction of insulin resistant patients from developing type 2 diabetes, the coincident hyperamylinemia leads to proteotoxicity and amyloid deposition in pancreatic islets. We show that amylin oligomers, fibrils and plaques also accumulate in failing hearts from obese and diabetic patients, but not in nonfailing hearts and failing hearts from lean, nondiabetic humans. Using rats transgenic for human amylin, we show that cardiac amylin oligomer accumulation causes myocyte Ca^{2+} dysregulation, activation of Ca^{2+}-dependent pathological cardiac hypertrophy and remodeling, and diastolic dysfunction. Our data suggest that cardiac amylin accumulation accelerates the onset of diabetic cardiomyopathy. The present results show for the first time that amylin oligomers are a direct pathogenic link between pancreatic and cardiac disorders and an independent contributor to the multifactorial pathogenesis of diabetic cardiomyopathy. We propose that detection and disruption of cardiac amylin buildup may be a predictor of myocardial dysfunction and a novel therapeutic target in diabetic cardiomyopathy.

<center>**SUPPLEMENTAL MATERIAL**</center>

Detailed Methods

Human tissue specimens
Heart specimens were obtained at the time of orthotopic heart transplantation at the Hospital of University of Pennsylvania (for failing hearts) or organ donation (for non-failing hearts) in accordance with the Institutional Review Board approval. Inclusion in tissue-based studies was not restricted on the basis of age, gender, race or ethnic status. Heart failure etiology, body mass index (BMI), age, gender and state of diabetes with respect to dependence on insulin and/or oral hypoglycemic agents of all cases studied here are summarized in the Supplemental Table.

Human heart tissues were divided in pathologically distinct groups as follows. DM-HF represents the group of failing hearts (HF) from patients with overt type-2 diabetes (DM) pre-transplantation (N=25). Both ischemic (ICM) and congestive (DCM) failing hearts were included in the study (Table). With few exceptions, patients in this group were either overweight, i.e. $25 \leq$ BMI <30, (N=7) or obese, i.e. BMI $\geq$30, (N=14), at the date of heart transplant. Some patients in this group were in an advanced stage of diabetes, as they received insulin (N=17). No patient included had a history of ketoacidosis. Other patients in the diabetes group received oral hypoglycemic agents alone (N=6), prior to heart transplant. OW/OB-HF stands for failing hearts from overweight/obese (OW/OB) patients, i.e. BMI $\geq$25, (N=8). Patients in this group presented severely impaired glucose tolerance in response to steroid exposure at the time of heart transplant and developed overt diabetes within 1 year post-transplantation. The OW/OB-NF group (N=8) includes non-failing hearts (NF) from overweight/obese individuals. Heart samples from lean (L), healthy patients without heart failure, i.e. the L-NF group (N=5), and from lean patients with heart failure but no diabetes, i.e. the L-HF group (N=7), served as controls. The L-HF group corresponds to patients with advanced chronic HF of variable duration (range 0.5 to 8 years) and included both individuals with ischemic and nonischemic etiologies for their HF, as shown in Supplemental Table 1.

Experimental Animals
Animal studies were approved by the University of California, Davis Animal Research Committee. Because rodent amylin is not amyloidogenic and rodents do not accumulate amylin amyloids (1), most rodent models are not adequate for this study. We used Sprague-Dawley rats that express human amylin in the pancreatic β-cells on the insulin II promoter (HIP rats) (2). HIP rat breeding pairs were kindly provided by Pfizer. These rats show amylin deposits in pancreatic islets and gradual decline in β-cell mass leading to impaired fasting glucose at 5 months of age and diabetes by 10 months of age (3). As negative controls, we used obese, insulin resistant rats expressing only the native, non-amyloidogenic rat amylin isoform, which does not form amyloids (UCD-T2DM rats) (4-7). The UCD-T2DM rat model was obtained by breading obese Sprague-Dawley rats with Zucker Diabetic Lean rats that have inherent ß-cell defects (4). UCD-T2DM rats exhibit hyperinsulinemia associated with insulin resistance prior to the onset of diabetes (4), similar to HIP rats and humans (2). The model was used for studies of pharmacological and surgical prevention and treatment of type-2 diabetes (5-7). Both HIP and UCD-T2DM rats develop diabetes on a similar time scale, as shown by longitudinal measurements of the pancreatic secretory function reported previously (2-4). In the present study, we used age matched HIP and UCD-T2DM rats in the pre-diabetic state, i.e. *non-fasting* (random) blood glucose level <200 mg/dl. Pre-diabetic male HIP (N=17) and UCD-T2DM

(N=19) rats were used for experiments. Wild-type littermates (N=16) served as non-diabetic controls for HIP rats. Age-matched SD rats (N=13, Charles Rivers Laboratory) were controls for UCD-T2DM rats.

Immunochemistry

Left ventricular tissue was homogenized in homogenization buffer containing 10 mmol/L Tris-HCl, pH 7.4, 150 mmol/L NaCl, 0.1% sodium dodecyl sulfate, 1% TritonX-100, 1% sodium deoxycholate, 5 mmol/L EDTA, 1 mmol/L NaF, 1 mmol/L sodium orthovanadate and protease and phosphatase inhibitor cocktail (Calbiochem). Isolated cardiac mocytes were lysed in lysis buffer containing 1% NP-40, 150 mM NaCl, 10 mM Tris-HCl, 2 mM EGTA, 50 mM NaF and protease and phosphatase inhibitor cocktail (Calbiochem). Blood samples were centrifuged at 3500 rpm to remove cellular components. Human samples were incubated with Protein A-coated magnetic beads (Invitrogen) for 6 hours to remove IgG, a possible source of cross-reactivity. Standard Western blot and dot blot experiments were performed. The following primary antibodies were used: polyclonal anti-amylin antibody (Peninsula) that recognizes both human amylin and rat amylin, polyclonal anti-BNP (Millipore), anti-SERCA monoclonal (clone 2A7-A1 from ABR), monoclonal anti-phospholamban (Badrilla) and polyclonal anti-Na/Ca exchanger (Millipore). For heart samples, equal loading was verified by re-probing with anti-GAPDH. Signal intensity analysis was performed in Image J. For each gel, we averaged the signal intensity of the corresponding bands for the control samples. Then, we normalized the signal intensity in all lanes to this average. This procedure was repeated on at least four gels and for each sample the normalized signal intensity was averaged. In the end, we calculated averages over all the groups used.

Immunohistochemistry was done on thin section from paraffin blocks using the same anti-amylin antibody and biotinylated goat anti-rabbit IgG (Vector) as the secondary antibody.

Cardiac insulin signaling

To determine the insulin responsiveness of the heart, rats were fasted overnight, injected (I.P.) with insulin (10 mU/g body weight) or saline, and sacrificed 10 min after injection. Hearts were excised quickly and frozen in liquid nitrogen. Immunoblots were performed on heart homogenates with phospho-Akt-Ser473, total Akt1/2, phospho-GSK3β-Ser9 and total GSK3β (Cell Signaling Danvers, MA). After gel electrophoresis, proteins were transferred on PVDF membranes, blocked and probed with primary antibodies against phospho-Akt-Ser473 or phospho-GSK3β-Ser9. After developing, membranes were stripped and re-probed with antibodies against total Akt and total GSK3β, respectively.

Cardiac myocyte isolation

Rats were anesthetized by I.P. injection of Nembutal (~1 mg/g) and hearts were excised quickly, placed on a Langendorff perfusion apparatus and perfused with 1 mg/ml collagenase (8). When the heart became flaccid, the left ventricular tissue was cut into small pieces, filtered and [Ca] in the cell suspension was progressively increased to 1 mM (8). The standard Tyrode's solution used in these experiments contained (in mM): 140 NaCl, 4 KCl, 1 $MgCl_2$, 10 glucose, 5 HEPES and 1 $CaCl_2$ (pH=7.4). All experiments were done at room temperature (23-25°C).

Intracellular Ca^{2+} measurements

Myocytes were plated on laminin-coated coverslips, mounted on the stage of a fluorescence miscroscope and loaded with Fura-AM or Fluo4-AM (10 μmol/L, for 35 min for both). Fura was alternately excited at 340 (F_{340}) and 380 nm (F_{380}) and emission was collected at 510±20 nm. Fluo-4 was excited at 488 nm and fluorescence collected at 535±30 nm. Data collected with

Fura-2 are expressed as the F_{340}/F_{380} ratio and Fluo4 data are expressed as F/F_0, where F_0 is the fluorescence signal in resting myocytes. Ca^{2+} transients were elicited by stimulation with external electrodes at frequencies between 0.2 and 2 Hz. The passive trans-sarcolemmal Ca^{2+} leak was measured as the initial rate of $[Ca^{2+}]_i$ declines upon reducing external Ca^{2+} from 1 to 0 mM. Ca^{2+} fluxes to and from the SR were blocked by pre-treating the cells with 10 μM thapsigargin for 10 min whereas the Na/Ca exchanger and sarcolemmal Ca^{2+}-ATPase were abolished by using $0Na^+/0Ca^+$ solution (Na^+ replaced with Li^+) and adding 20 μM carboxyeosin, respectively.

Activation of Ca^{2+}-dependent hypertrophic pathways

Activation of Ca^{2+}/calmodulin-dependent protein kinase II-histone deacetylase (HDAC) and calcineurin- nuclear factor of activated T cells (NFAT) hypertrophic pathways was examined by determining the nuclear *vs*. cytosolic localization of HDAC4 and NFATc4 in cardiac myocytes. Cells freshly isolated from pre-diabetic HIP and age-matched WT rats were plated on laminin-coated coveslips, fixed with paraformaldehyde, permeabilized with 0.2% Triton-100, blocked with 2% goat serum and labeled with polyclonal primary antibodies against HDAC4 and NFATc4 (Santa Cruz Biotechnology). Anti-rabbit Alexa Fluor 488 was used as secondary antibody and fluorescence images were collected with a laser scanning confocal microscope. The ratio of the average fluorescence signal in the nucleus *vs*. cytosol was calculated with Image J.

In vivo echocardiography and hemodynamics

The rats were anesthetized with 50 mg/kg ketamine and 5 mg/kg xylazine, their chests were shaved, and an echocardiogram was done (Acuson, Sequoia model C512, 15-MHz probe) (9). Two-dimensional imaging was used to identify the short-axis position. Three consecutive m-mode images were collected in the short-axis view and saved for analysis of chamber size and fractional shortening. In an animal subset, while the rat was under anesthesia, a carotid artery catheter was passed into the left ventricle to assess pressure/volume loops (9). Fractional shortening, heart rate, ventricular pressure, cardiac output, dP/dt, stroke work and pressure/volume loops were measured.

Electron microscopy

To visualize the nature of the molecular entities formed by human and rat amylin at 50μM peptide concentration in serum, aliquots of each aggregation reaction were imaged by a Philips CM 12 electron microscope (10). The aliquots were deposited onto freshly glow-discharged carbon films. The carbon films were supported by lacy Formvar/carbon films on 200-mesh copper grids. Small sample drops were allowed to sit for 2 min on the carbon surfaces, and then excess fluid was blotted away. The carbon surfaces were then rinsed by applying 5-μL drops of deionized water for 1 min to remove the buffer. Finally, the samples were negatively stained by applying 5 μL of 1% uranyl acetate for 1 min. Electron microscopy images were recorded at 26,000× magnification.

Statistical Analysis

Data are expressed as mean ± SEM. Statistical discriminations were performed using two-tailed unpaired Student's t test, with $P < 0.05$ considered significant. One way analysis of variance (ANOVA) with the Dunnett post hoc test was used when comparing multiple groups.
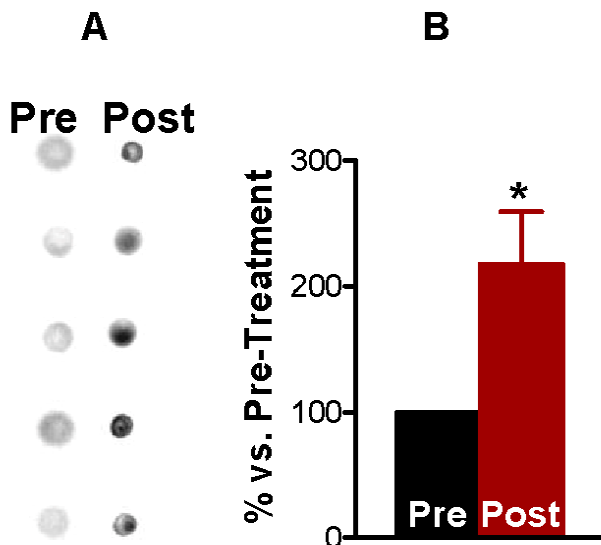
Online Figure I.
Negative control experiments aimed at testing the specificity of the bands identified in Western blot analysis in Fig 1. Duplicate samples were loaded onto a gel and after blotting and blocking, the membrane was cut and one half was incubated with the anti-amylin antibody while the other half was incubated in the absence of a primary antibody. Both halves were then incubated with the secondary antibody and developed and imaged together. The supplemental figure shows that there is no cross-reactivity with the secondary antibody.
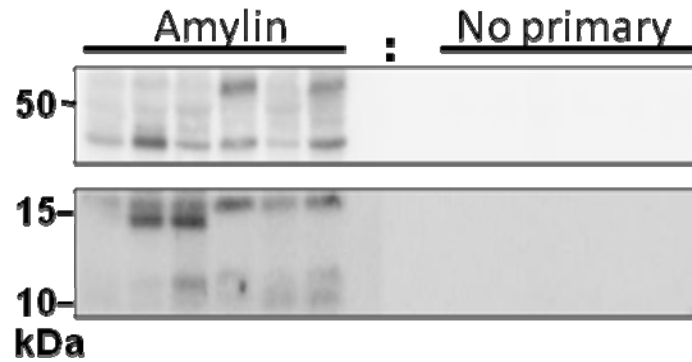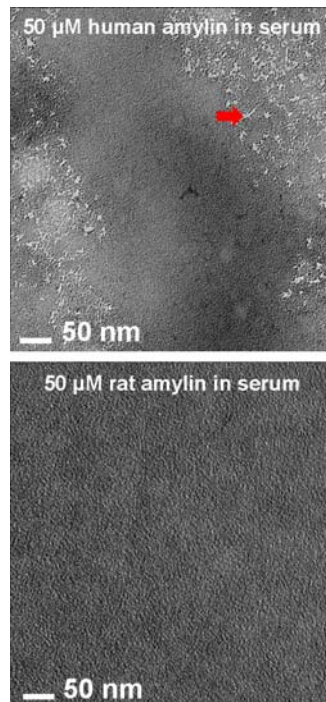
Online Figure II

To estimate the amylin content in insoluble fractions from human heart protein homogenates, pellets were treated with formic acid, freeze dried and then the resulting powders were re-suspended in guanidine hydrochloride. Dot blots with an anti-amylin antibody (**A**) showed significantly increased amylin levels in post-treatment versus pre-treatment samples (**B**). (P = 0.02, Student's t-test.) The test suggests that large amylin aggregates fragmented into small oligomers that were recognized by the anti-amylin antibody.
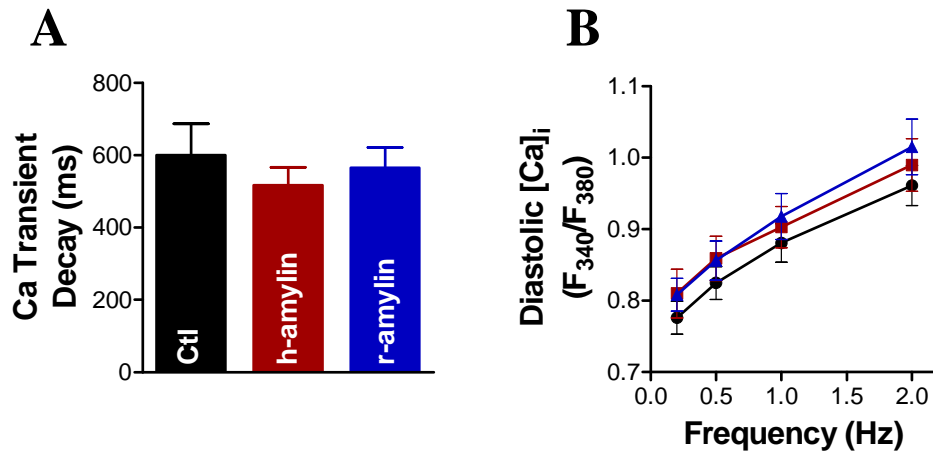
Online Figure III

Electron microscopy of amylin oligomer formation in serum. Electron microscopy images show that 50 μM *human* amylin incubated in serum for 1h has a faster oligomerization reaction than *rat* amylin and forms oligomers and protofibrils (arrow). Oligomerization of *human* amylin resulted in a marked rise in Ca^{2+} transient amplitude (see Fig.3).
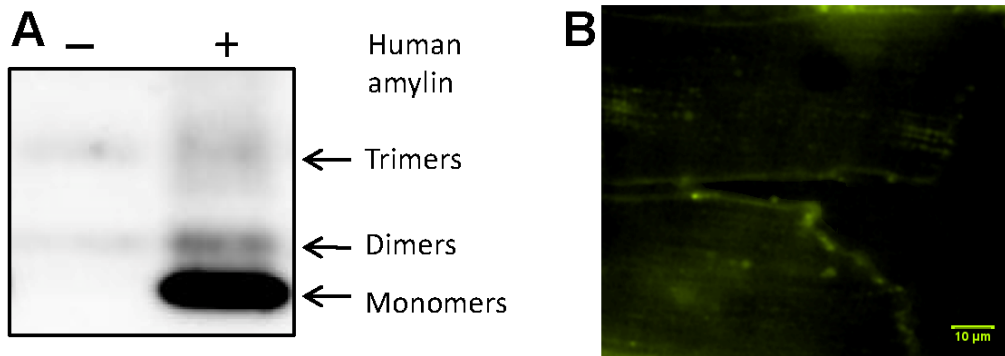
Online Figure IV

Ca^{2+} transient decay (A) and diastolic $[Ca^{2+}]_i$ (B) in control rat myocytes (Ctl) and myocytes pre-incubated for 1-2 hours with 50 µM human (h-amylin) or rat amylin (r-amylin).

A

B

Online Figure V

Human amylin attaches to cardiac myocyte sarcolemma.

(A) Isolated rat myocytes were incubated with 50 µmol/L human amylin (+) or with PBS (–) for 2 h at room temperature. Myocytes were then washed with PBS, lysed and immunoblots were performed with an anti-amylin antibody. The results show the presence of human amylin monomers, dimers and trimers in the group treated with human amylin. (B) Isolated rat myocytes were plated on glass coverslips and incubated with 20 µmol/L of fluorescent FAM-human amylin (AnaSpec) for 2 h. Myocytes were then washed and confocal fluorescence images were recorded. Data show fluorescence staining of the sarcolemma, indicating that human amylin binds to the myocyte membrane.
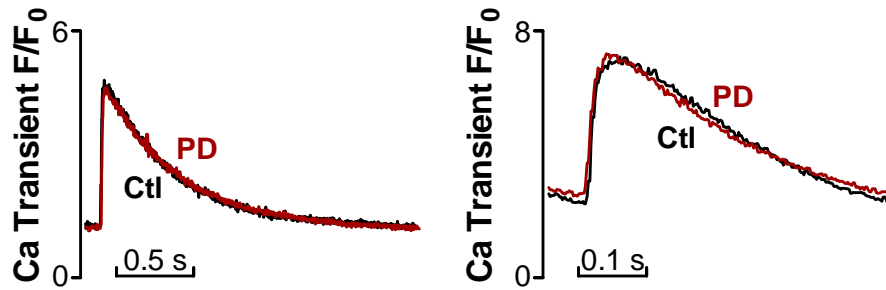
Online Figure VI

GSK-3β phosphorylation in hearts from pre-diabetic HIP and UCD-T2DM rats and littermate controls under basal conditions (0 insulin) and following stimulation with insulin (10 mU⁄g body weight). Representative example and mean values for the ratio between phosphorylated and total GSK-3β. N=3 rats for each group.
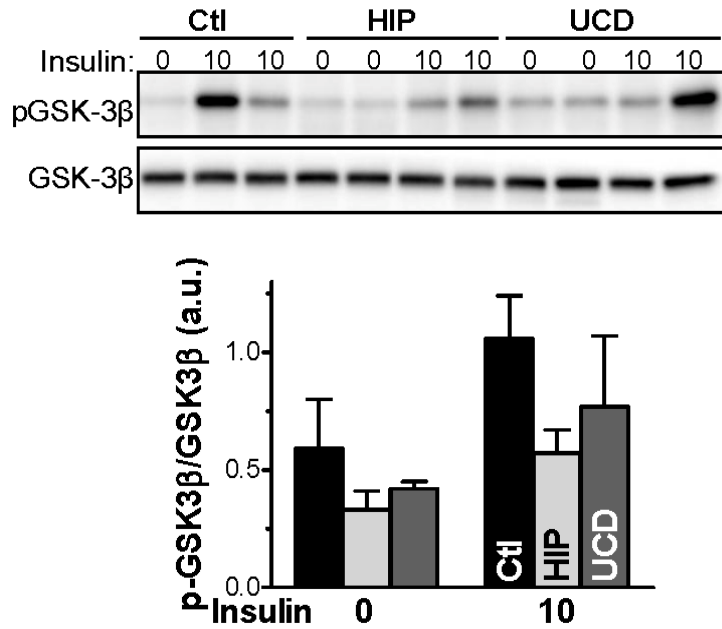
Online Figure VII

Representative Ca^{2+} transients in myocytes from control (Ctl) and pre-diabetic (PD) UCD-T2DM rats paced at 0.5 Hz and 2 Hz.

Online Figure VIII
Nuclear import of NFAT and unchanged HDAC distribution in rat myocytes incubated with 50 µmol/L human amylin for 2 h.
The top panels show representative images from control myocytes (untreated) and cells incubated with human amylin (H-amylin). The bottom panels show the quantification of the nuclear-to-cytosolic ratio for HDAC4 and NFATc4. Experiments were done on more than 12 cells for each group.
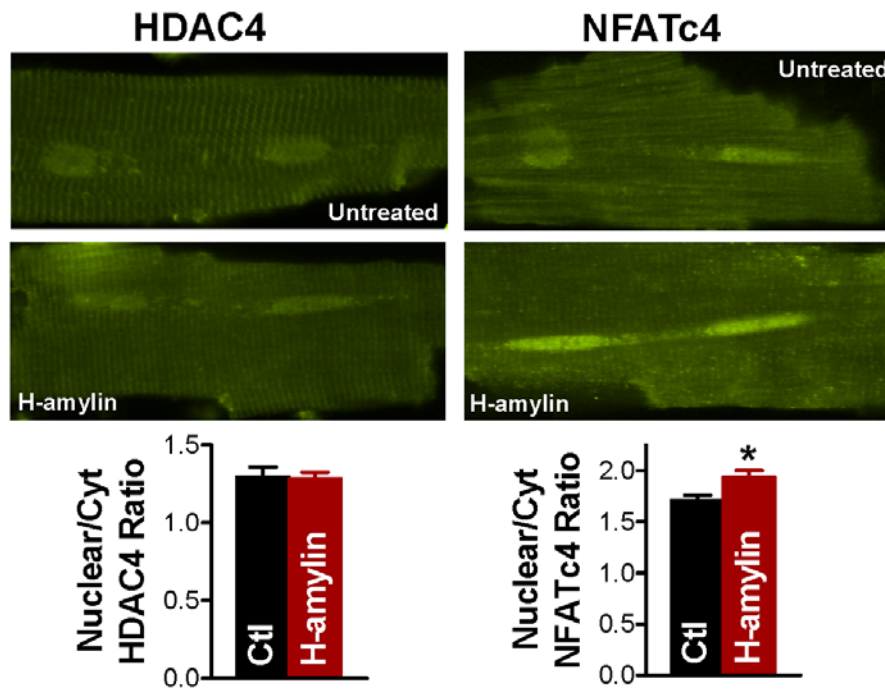
Online Figure IX
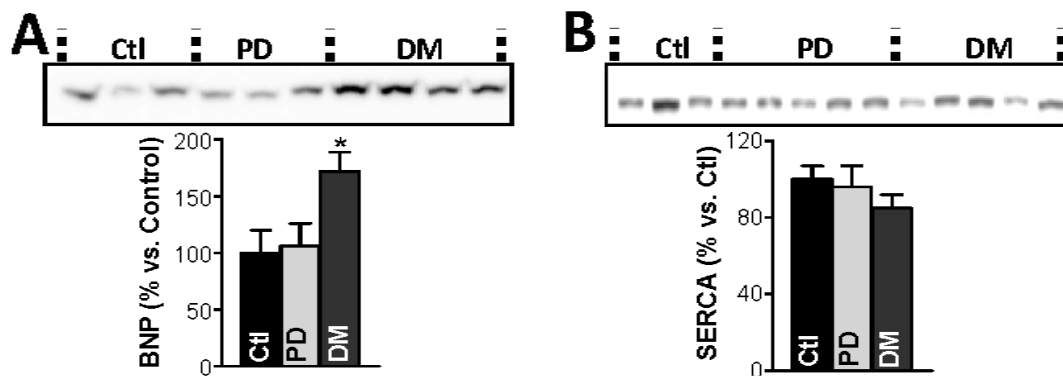BNP and SERCA levels in hearts from UCD-T2DM rats.
(A) BNP level is elevated in hearts from diabetic but not in pre-diabetic UCD-T2DM rats. (B)
SERCA expression is unchanged in hearts from pre-diabetic UCD-T2DM rats. Ctl – 5 hearts; PD
– 5 hearts, DM – 5 hearts.

Online Table I. Heart failure etiology, gender, age, BMI, and state of diabetes with respect to hyperglycemia and dependence of insulin and/or hypoglycemics for all patients from who heart tissue was used in this study.

Code	HF Etiology	Gender	Age	BMI
DM-HF (Insulin)	ICM	M	50	32
			58	25.7
			59	31.4
			64	36.6
			58	25.7
	DCM	F	61	28
			44	31.2
			43	40.3
		M	45	32.2
			54	28.6
			64	25.5
			59	27.7
			67	31.2
			56	32.1
			47	35.2
DM-HF (Hypoglycemics)	ICM	M	60	35
			66	20.6
			56	31
			60	20.6
			63	24.3
	DCM	M	38	32.1
			58	34
			66	23.1
			58	34
		F	58	28.4
OW/OB-HF	ICM	M	42	28
			58	22.7
			63	25.2
			54	23.8
			47	25.9
			63	24
			49	32.7
		F	54	29.4
OW/OB-NF		F	52	24.2
			51	28
			60	31.2
			51	31.9
			43	34.1

		M	50	31.8
			52	31.2
			59	28.7
L-NF		F	37	20.8
			33	24.3
		M	20	23.7
			45	25.1
			46	20.1
L-HF	ICM	M	48	19.7
			25	22.1
			58	22.7
	DCM	F	44	20.7
		M	57	23.9
			34	19.9
			46	21.8

Online References

1. Westermark P, Engström U, Johnson KH, Westermark GT, Betsholtz C. Islet amyloid polypeptide: pinpointing amino acid residues linked to amyloid fibril formation. *Proc. Natl. Acad. Sci. USA*. 1990;87:5036-5040.

2. Matveyenko AV, Butler PC. Islet amyloid polypeptide (IAPP) transgenic rodents as models for Type 2 Diabetes. *ILAR Journal*, 2006;47:225-233.

3. Matveyenko AV, Butler PC. β-cell deficit due to increased apoptosis in the human islet amyloid polypeptide transgenic (HIP) rat recapitulates the metabolic defects present in type-2 diabetes. *Diabetes* 2006;55:2106-2114.

4. Cummings BP, Digitale EK, Stanhope KL, Graham JL, Baskin DG, Reed BJ, Sweet IR, Griffen SC, Havel PJ. Development and characterization of a novel rat model of type 2 diabetes mellitus: the UC Davis type 2 diabetes mellitus UCD-T2DM rat. *Am. J. Physiol. Regul. Integr. Comp. Physiol.* 2008;295:R1782-1793.

5. Cummings BP, Stanhope KL, Graham JL, Baskin DG, Griffen SC, Nilsson C, Sams A, Knudsen LB, Raun K, Havel PJ. Chronic administration of the glucagon-like peptide-1 analog, liraglutide, delays the onset of diabetes and lowers triglycerides in UCD-T2DM rats. *Diabetes* 2010;59:2653-2661.

6. Cummings BP, Strader AD, Stanhope KL, Graham JL, Lee J, Raybould HE, Baskin DG, Havel PJ. Ileal interposition surgery improves glucose and lipid metabolism and delays diabetes onset in the UCD-T2DM rat. *Gastroenterology* 2010;138:2437-2446.

7. Cummings BP, Bettaieb A, Graham JL, Stanhope KL, Dill R, Morton GJ, Haj FG, Havel PJ. Subcutaneous administration of leptin normalizes fasting plasma glucose in obese type 2 diabetic UCD-T2DM rats. *Proc Natl Acad Sci U S A* 2011;108:14670-1475.

8. Despa S, Bers DM. Functional analysis of Na/K-ATPase isoform distribution in rat ventricular myocytes. *Am J Physiol - Cell Physiol* 2007;293:C321-C327.

9. Lin L, Kim SC, Wang Y, Gupta S, Davis B, Simon SI, Torre-Amione G, Knowlton AA. HSP60 in heart failure: abnormal distribution and role in cardiac myocyte apoptosis. *Am. J. Physiol. Heart Circ. Physiol.* 2007;293:H2238-H2247.

10. Walton JH, Berry RS, Despa F, Amyloid oligomer formation probed by water proton magnetic resonance spectroscopy. *Biophys. J.* 2010;100:2302-2308.